

MAGNETIC FIELD DISTRIBUTION IN THE ROTOR OF PERMANENT MAGNETS

I. Bucenieks, R. Krishbergs, K. Kravalis, G. Lipsbergs, A. Shishko
Institute of Physics, University of Latvia, 32 Miera str., LV-2169 Salaspils, Latvia
(imants@sal.lv)

Introduction. Due to rapid progress in last two decades in developing new rear earth magnetic materials allowing to produce very strong permanent magnets, wider interest arises in using them in different MHD devices for generating alternating traveling and/or rotating magnetic fields instead of traditional 3-phase inductors. The advantages of inductors (rotors) with permanent magnets poles are obvious. First of all, the inductor on permanent magnets has a higher efficiency, as there is no need to waste energy for generating the magnetic field. Second, inductors on permanent magnets have no windings at all and from this fact another important advantages follow: a simpler design, smaller overall dimensions and weight.

At the Institute of Physics of the University of Latvia series of electromagnetic induction pumps on permanent magnets [1] for different liquid metals applications have been developed, covering a rather wide range of developed pressure and provided flow rates. Additionally, theoretical investigations demonstrated that such permanent magnet inductors may be successfully used for producing flat induction MHD stoppers in devices for steel strip galvanizing [2].

In this report the results of analytical calculations of a two-dimensional magnetic field generated by a system of linear permanent magnets fixed on the inner ferrous base in an annular nonmagnetic gap are presented. All physical parameters of linear permanent magnets are identical and the magnetization of each magnet of rectangular form is considered to be uniform and constant. The calculated distribution of the magnetic field generated by an 8-poles inductor is compared with the results of measurements on the model.

1. Analytical calculations. In the report the analytical calculations of the magnetic field generated by a periodic system of permanent magnets in the annular gap for rotors with a radial working magnetic field component, Fig. 1a, are considered.

Let us assume that the length of rotors is long enough and the magnetic field in the nonmagnetic gap can be considered as two-dimensional (no axial components of the magnetic field). Let us take $N = 2p$ – the number of linear permanent magnets fixed on an inner ferrous yoke (p – number of poles pairs), R_0 – radius of the rotor, R_f – radius of an outer ferrous yoke. We consider that magnetization \mathbf{M} for all rectangular magnets (having cross-section $h_m a_m$) is the same and uniform ($|\mathbf{M}| = B_r = \text{const}$) and does not depend on magnetic fields generated by other magnets. Here h_m is the height of linear magnet in the direction of magnetization and a_m is its width. According to the theory of magnetism [3], such linear magnet is equivalent to the system of two surface electric currents with opposite directions and having density $J_s = B_r/\mu_0$ and passing through the side surfaces of magnets.

In the cylindrical coordinate system the periodicity of structure allows to consider the task only in the sector: $0 \leq \varphi \leq \alpha = \pi/2p$. As a scale of length, we take a radius R_0 , then $h = h_m/R_0$, $a = a_m/R_0$ and $R = R_f/R_0$, Fig. 1b. The equation of side surface will be: $\beta_s(\rho) = \arcsin(a/2\rho)$, where $r \leq \rho \leq 1$, $r = \sqrt{(1 - 2h \cdot \sqrt{(1 - (a/2)^2}) + h^2)}$.

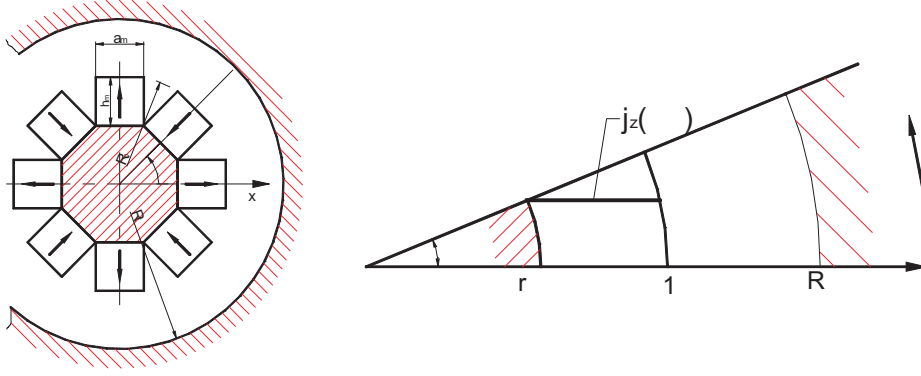


Fig. 1. Cross-section of an 8-pole magnetic rotor and the schematic of calculation region: $0 \leq \varphi \leq \alpha$; $r \leq \rho \leq R$, $\alpha = 22.5^\circ$.

It is easy to show that the distribution of current density in our system of coordinates can be expressed by the following expressions:

$$j_z(\rho, \varphi) = \frac{J_s}{R_0 \rho} \cdot \frac{\delta(\varphi - \beta_s(\rho))}{\sqrt{1 - (a/2\rho)^2}}, \quad \text{at } r \leq \rho \leq 1,$$

and $j_z(\rho, \varphi) = 0$, $\rho < r$, $\rho > 1$.

The magnetic field is calculated using the z -component of vector potential $A_z(\rho, \varphi)$ having components $B_\rho = \frac{1}{R_0 \rho} \frac{\partial A_z}{\partial \varphi}$ and $B_\varphi = -\frac{1}{R_0} \frac{\partial A_z}{\partial \rho}$, which should correspond to the following boundary problem:

$$\frac{\partial^2 A_z}{\partial \rho^2} + \frac{1}{\rho} \frac{\partial A_z}{\partial \rho} + \frac{1}{\rho^2} \frac{\partial^2 A_z}{\partial \varphi^2} = -\mu_0 R_0^2 j_z(\rho, \varphi)$$

$$0 \leq \varphi \leq \alpha, \quad \varphi = 0: \partial A_z / \partial \rho = 0; \quad \varphi = \alpha: \partial A_z / \partial \varphi = 0.$$

On the surface of the outer ferrous yoke (with $\mu = \infty$) at $\rho = R$ we have $\partial A_z / \partial \varphi = 0$. To simplify the task, the same condition was used also at the boundary $\rho = r$: $\partial A_z / \partial \varphi = 0$. So the surface of the inner ferrous polygonal-shaped yoke is substituted by the cylindrical surface. It is clear that an error introduced by this simplification is minimized at increasing the number of poles N and the height of linear magnets a_m . As an analytical solution of the boundary problem is solved by tailoring solutions in regions $r \leq \rho \leq 1$ and $1 \leq \rho \leq R$, at the boundary $\rho = 1$ the condition of discontinuity of the potential and its derivative $\partial A_z / \partial \rho$ are used. As a result, a solution of the boundary problem is represented in the following way at $r \leq \rho \leq 1$:

$$A_z(\rho, \varphi) = \frac{2R_0 B_r}{\pi} \sum_{k=1}^{\infty} A_k(\rho) \frac{\sin(2k-1)p\varphi}{2k-1},$$

where

$$\begin{aligned}
 A_k(\rho) = & \int_r^\rho (t/\rho)^{(2k-1)p} \cdot \frac{\sin [(2k-1)p \arcsin(a/2t)]}{\sqrt{1-(a/2t)^2}} dt + \\
 & + \int_\rho^1 (\rho/t)^{(2k-1)p} \cdot \frac{\sin [(2k-1)p \arcsin(a/2t)]}{\sqrt{1-(a/2t)^2}} dt + \\
 & + \frac{1}{1-(r/R)^{2(2k-1)p}} \int_r^1 \left\{ \left(\frac{r^2}{\rho t}\right)^{(2k-1)p} + \left(\frac{\rho r^2}{tR^2}\right)^{(2k-1)p} + \right. \\
 & \left. + \left(\frac{t\rho}{R^2}\right)^{(2k-1)p} \left[1 + \left(\frac{r^2}{\rho^2}\right)^{(2k-1)p}\right] \right\} \times \frac{\sin [(2k-1)p \arcsin(a/2t)]}{\sqrt{1-(a/2t)^2}} dt;
 \end{aligned}$$

At the boundary conditions $1 \leq \rho \leq R$ we have:

$$\begin{aligned}
 A_z(\rho, \varphi) = & \frac{2R_0 B_r}{\pi} \sum_{k=1}^{\infty} B_k \left[\rho^{-(2k-1)p} + \left(\frac{\rho}{R^2}\right)^{(2k-1)p} \right] \frac{\sin(2k-1)p\varphi}{(2k-1)}, \quad \text{where} \\
 B_k = & \frac{1}{1-\left(\frac{r}{R}\right)^{2(2k-1)p}} \int_r^1 \left[t^{(2k-1)p} + \left(\frac{r^2}{t}\right)^{(2k-1)p} \right] \frac{\sin [(2k-1)p \arcsin(a/2t)]}{\sqrt{1-(a/2t)^2}} dt.
 \end{aligned}$$

For practice, the distribution of the magnetic field is of interest in the region of the nonmagnetic gap at $1 \leq \rho \leq R$:

$$\begin{aligned}
 B_\rho(\rho, \varphi) = & \frac{2pB_r}{\pi} \sum_{k=1}^{\infty} B_k \left[\rho^{-(2k-1)p} + \left(\frac{\rho}{R^2}\right)^{(2k-1)p} \right] \frac{\cos(2k-1)p\varphi}{\rho}, \\
 B_\varphi(\rho, \varphi) = & \frac{2pB_r}{\pi} \sum_{k=1}^{\infty} B_k \left[\rho^{-(2k-1)p} - \left(\frac{\rho}{R^2}\right)^{(2k-1)p} \right] \frac{\sin(2k-1)p\varphi}{\rho}.
 \end{aligned}$$

The absence of the outer ferrous yoke means that in all the above formulae R should be set infinite.

2. Comparison of calculation and experimental results. The results of theoretical calculations were compared with the results of measurements of the magnetic field distribution for the real experimental model of the 8-pole

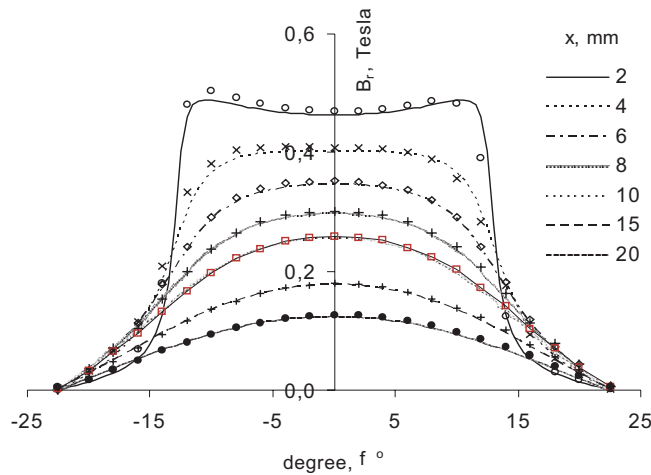


Fig. 2. Comparison of calculation results with experimental measurements.

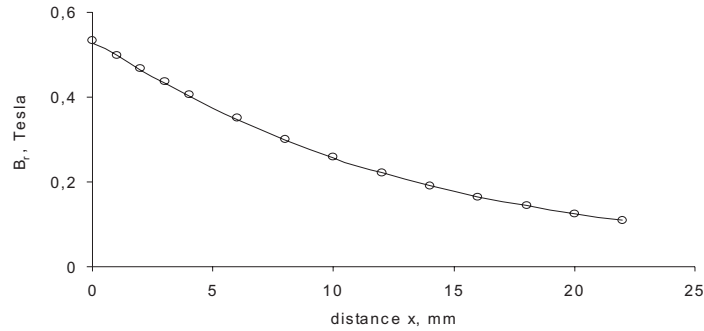


Fig. 3. Dependence of the radial component of the magnetic field on the distance from the pole surface.

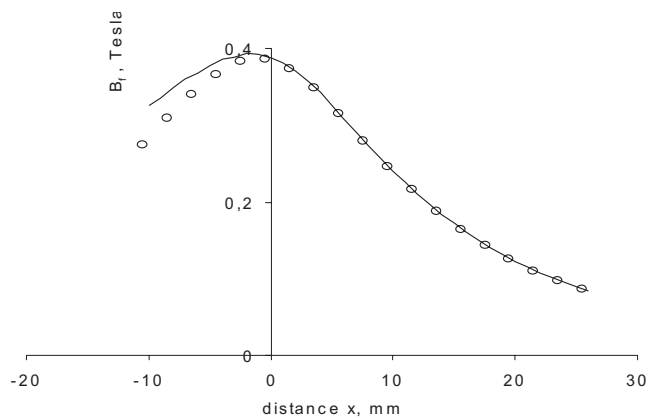


Fig. 4. Distribution of the azimuthal component of the magnetic field.

rotor ($p = 4$), Fig. 1, of length 250 mm and assembled from permanent NdFeB magnets with the square cross-section $a_m = h_m = 25$ mm, length 50 mm with inside magnetization $B_r = 1.1$ Tesla. The outer passive ferrous yoke was absent that corresponds to $R_f = \infty$. The radius of the rotor was $R_0 = 56.4$ mm.

In Fig. 2 the comparison of the results of calculations and the results of experimental measurements of the magnetic field distribution for the radial component depending on azimuth at different distances x from the surface of the rotor is illustrated (the distance x is measured from the pole surface located at the distance 55 mm from the rotor axis). In Fig. 3 the dependence of the radial component of the magnetic field on the distance x at $\varphi = 0$ is illustrated. The dependence of the azimuthal component on the distance x in the plane $\varphi = \alpha$ between the magnets is illustrated in Fig. 4.

3. Conclusion. Comparison of the results of calculations with the results of experimental measurements for the magnetic field distribution generated by the rotor demonstrates that the formulae derived from the analytical solution give a rather good agreement.

REFERENCES

1. I. BUCENIĲKS. Perspectives of using rotating permanent magnets for electromagnetic induction pump design. *Magnetohydrodynamics*, vol. 36 (2000), no. 2, pp. 151–156.
2. J. VALDMANIS, R. KRISBERGS, A. SHISHKO. Rotating permanent magnets MHD seal. *Magnetohydrodynamics*, vol. 39 (2003), no. 4, pp. 435–443.
3. E. PURCELL. Electricity and magnetism. *Berkley Physics Course*, vol. 2, p. 439.